Rigid Rod-Like Dinuclear Ru(II)/Os(II) Terpyridine-Type Complexes. Electrochemical Behavior, Absorption Spectra, Luminescence Properties, and Electronic Energy Transfer through Phenylene Bridges

Francesco Barigelletti,*[1a] Lucia Flamigni,[1a] Vincenzo Balzani,*[1b] Jean-Paul Collin,*[1c] Jean-Pierre Sauvage,*[1c] Angelique Sour,[1c] Edwin C. Constable,*[1d] and Alexander M. W. Cargill Thompson[1d]

Contribution from Istituto FRAE-CNR, 40129 Bologna, Italy, Dipartimento di Chimica "G. Ciamician", Università di Bologna, 40126 Bologna, Italy, Laboratoire de Chimie Organo-Minerale, Institut de Chimie, Université L. Pasteur, 67000 Strasbourg, France, and Institut für Anorganische Chemie, Universität Basel, 4056 Basel, Switzerland

Received April 4, 1994[⊗]

Abstract: The absorption spectra, the luminescence properties (at 293 and 77 K), and the electrochemical behavior of six dinuclear heterometallic compounds have been investigated. The compounds are made of $Ru(tpy)_2^{2+}$- and $Os(tpy)_2^{2+}$-type components (tpy = 2,2′:6′,2″-terpyridine, which in some cases carries *p*-tolyl (Meph) or methylsulphone (MeO_2S) substituents in the 4′ position), connected by *n* phenylene (ph) spacers (*n* = 0, 1, and 2). In the resulting rigid rod-like structures of general formula $(X_1tpy)Ru(tpy(ph)_ntpy)Os(tpyX_2)^{4+}$ the metal-to-metal distance varies from 11 to 20 Å. The absorption spectra of the two components are slightly perturbed in the dinuclear compounds, and metal–metal and ligand–ligand interactions are evidenced by the trends of the oxidation and reduction potentials. The luminescence of the Ru-based unit is quenched by the connected Os-based unit with practically unitary efficiency, regardless of the number of interposed phenylene spacers. Quenching is accompanied by quantitative sensitization of the Os-based luminescence. The rate of energy transfer at 293 K is larger than 10^{10} s^{-1} in all cases. The Förster (Coulombic) mechanism does not satisfactorily account for such a fast rate, particularly for the species with *n* = 2. It is concluded that the observed energy-transfer processes take place most likely via a Dexter (electron exchange) mechanism. This is consistent with the strong electronic coupling of the Ru-based and Os-based units in the compound with *n* = 0, and with the relatively small insulating effect expected for the phenylene spacers.

Introduction

The design of nanomachines and the bottom-up construction of miniaturized components capable of performing specific functions are important challenges facing modern chemistry.[2-5] Progress in this field requires the availability of molecular components (building blocks) having well-defined *structures and properties*. As far as light- and/or redox-induced functions are concerned, much attention is presently focused on systems based on $M(N-N)_3^{n+}$ building blocks, where M is a metal ion of the second or third transition row (in particular, Ru(II) and Os(II)) and N–N is a bidentate bpy-type ligand (bpy = 2,2′-bipyridine).[6] This choice is justified by the outstanding excited-state and redox properties of the $M(bpy)_3^{n+}$-type complexes.[7] In terms of structure, however, the use of bidentate bpy-type ligands is not ideal for two reasons: (1) stereo and/or geometric isomers are present since bidentate ligands (a) give rise to stereoisomerism at six-coordinated centers, and (b) if they bear a single substituent, two geometrical isomers with *facial* and *meridional* arrangement can be formed; (2) the building up of supramolecular species with the basic $M(bpy)_3^{n+}$ arrangement occurs with no control of isomer formation when singly substituted bpyX ligands are used; therefore, if both an electron donor D and an electron acceptor A are to be linked to a $M(bpy)_3^{n+}$ unit, a mixture of *cis*- and *trans*-type triad systems are obtained.

The use of tridentate tpy-type ligands (Scheme 1; tpy = 2,2′:6′,2″-terpyridine) is much more convenient from a geometric viewpoint.[8-10] $M(tpy)_2^{n+}$ complexes are in fact achiral, and the introduction of a single substituent in the 4′ position of each tpy ligand does not cause isomerism problems and offers the possibility of designing triads in which the two additional components lie in opposite directions with respect to the photosensitizer.[11,12]

The price to pay on replacing bpy-type with tpy-type ligands in Ru(II) complexes is a shorter excited-state lifetime and a much weaker luminescence intensity in fluid solution at room temperature.[10] A systematic investigation of $Ru(tpy)_2^{2+}$-type com-

⊗ Abstract published in *Advance ACS Abstracts*, July 15, 1994.

(1) (a) Istituto FRAE-CNR. (b) Università di Bologna. (c) Université Louis Pasteur, Strasbourg. (d) Universität Basel.

(2) Lehn, J.-M. *Angew. Chem., Int. Ed. Engl.* **1990**, *29*, 1304.

(3) Balzani, V.; Scandola, F. *Supramolecular Photochemistry*; Horwood: Chichester, 1991; Chapter 12.

(4) (a) *Molecular Electronic Devices*; Carter, F. L., Siatkowsky, R. E., Woltjien, H., Eds.; North Holland; Amsterdam, 1988. (b) Drexler, K. E. *Nanosystems: Molecular Machinery, Manufacturing and Computation*; Wiley: New York, 1992.

(5) Ballardini, R.; Balzani, V.; Gandolfi, M. T.; Prodi, L.; Venturi M.; Philip, D.; Ricketts, H. G.; Stoddart, J. F. *Angew. Chem., Int. Ed. Engl.* **1993**, *32*, 1301.

(6) (a) Scandola, F.; Indelli, M. T.; Chiorboli, C.; Bignozzi, C. A. *Top. Curr. Chem.* **1990**, *158*, 73. (b) Reference 3, Chapters 5 and 6. (c) Denti, G.; Campagna, S.; Balzani, V. In *Mesomolecules: from Molecules to Materials*; Mendenhall, G. D., Greenberg, A., Liebman, J., Eds.; Chapman and Hall: New York, in press.

(7) (a) Meyer, T. J. *Pure Appl. Chem.* **1986**, *58*, 1193. (b) Juris, A.; Balzani, V.; Barigelletti, F.; Campagna, S.; Belser, P.; von Zelewsky, A. *Coord. Chem. Rev.* **1988**, *84*, 85. (c) Kalyanasundaram, K. *Photochemistry of Polypyridine and Porphyrin Complexes*; Academic Press: London, 1991.

(8) Collin, J.-P.; Guillerez, S.; Sauvage, J.-P. *J. Chem. Soc., Chem. Commun.* **1989**, 776.

(9) (a) Constable, E. C.; Cargill Thompson, A. M. W. *J Chem. Soc., Dalton Trans.* **1992**, 3467. (b) Constable, E. C.; Cargill Thompson, A. M. W.; Tocher, D. A. *Supramolecular Chemistry*; Balzani, V., De Cola, L. Eds.; Kluwer: Dordrecht, 1992; p 219.

(10) Sauvage, J.-P.; Collin, J.-P.; Chambron, J.-C.; Guillerez, S.; Coudret, C.; Balzani, V.; Barigelletti, F.; De Cola, L.; Flamigni, L. *Chem. Rev.* **1994**, *94*, 993.

(11) Collin, J.-P.; Guillerez, S.; Sauvage, J.-P.; Barigelletti, F.; De Cola, L.; Flamigni, L.; Balzani, V. *Inorg. Chem.* **1991**, *30*, 4230.

(12) Collin, J.-P.; Guillerez, S.; Sauvage, J.-P.; Barigelletti, F.; De Cola, L.; Flamigni, L.; Balzani, V. *Inorg. Chem.* **1992**, *31*, 4112.

0002-7863/94/1516-7692$04.50/0

Scheme 1

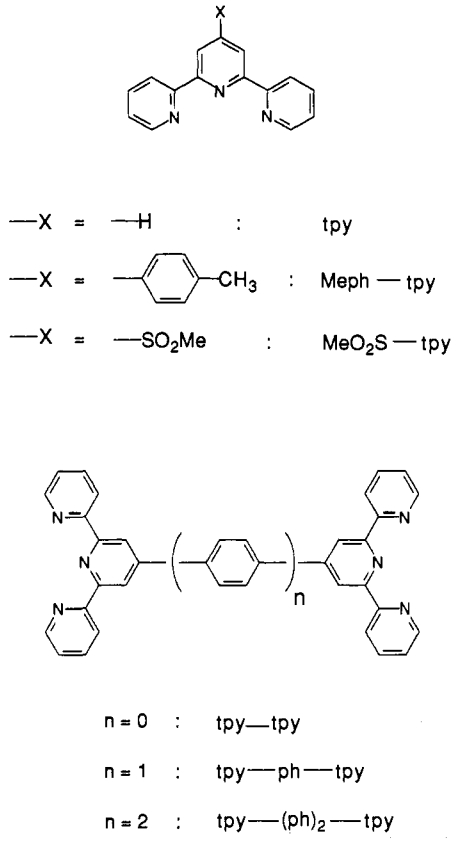

plexes, however, has recently shown that this drawback can be at least in part overcome by using appropriate substituents (e.g., $MeSO_2$) on the tpy ligand.[13]

Taking advantage of the structural properties of the $M(tpy)_2^{n+}$-type complexes, we have synthesized a series of rigid, rod-like compounds (Scheme 1, Figure 1) where Ru(II)-based and Os(II)-based building blocks are either directly linked or connected by one or two phenylene spacers.[14] In such systems the metal-to-metal distance is 11, 15.5, or 20 Å, depending on the number (n) of interposed *para*-phenylene spacers (n = 0, 1, or 2, respectively). Because of the well-known energy difference between the lowest excited states of Ru(II) and Os(II) tpy-type complexes,[7] electronic energy transfer is expected to occur from the Ru-based to the Os-based unit.

We report here the results of an investigation of the excited-state and redox properties of the prepared compounds.[15] Energy transfer has been monitored by using stationary and time-resolved luminescence spectroscopy. The role of the phenylene spacer, which has been recently investigated in other systems,[16-18] is discussed, and it is shown that the electron exchange (Dexter) mechanism is responsible for the highly efficient energy transfer from the Ru-based to the Os-based component.

(13) (a) Constable, E. C.; Cargill Thompson, A. M. W.; Armaroli, N.; Balzani, V.; Maestri, M. *Polyhedron* **1992**, *20*, 2707. (b) Constable, E. C.; Cargill Thompson, A. M. W.; Armaroli, N.; Balzani, V.; Maestri, M. Manuscript in preparation.

(14) Similar rod-like complexes based on Ru(II), Cu(I), or Fe(II) metals have been recently prepared by Grosshenny and Ziessel: (a) Grosshenny, V.; Ziessel, R. *J. Chem. Soc., Dalton Trans.* **1993**, 817. (b) *J. Organomet. Chem.* **1993**, *453*, C19.

(15) For preliminary results on some of these compounds, see: Barigelletti, F.; Flamigni, L.; Balzani, V.; Collin, J.-P.; Sauvage, J.-P.; Sour, A.; Constable, E. C.; Cargill Thompson, A. M. W. *J. Chem. Soc., Chem. Commun.* **1993**, 942.

(16) Kim, Y.; Lieber, C. M. *Inorg. Chem.* **1989**, *28*, 3990.

(17) (a) Osuka, A.; Satoshi, N.; Maruyama, K.; Mataga, N.; Asahi, T.; Yamazaki, I.; Nishimura, Y.; Onho, T.; Nozaki, K. *J. Am. Chem. Soc.* **1993**, *115*, 4577. (b) Osuka, A.; Maruyama, K.; Mataga, N.; Asahi, T.; Yamazaki, I.; Tamai, N. *Ibid.* **1990**, *112*, 4958.

(18) (a) Helms, A.; Heiler, D.; McLendon, G. *J. Am. Chem. Soc.* **1991**, *113*, 4325. (b) *Ibid.* **1992**, *114*, 6227.

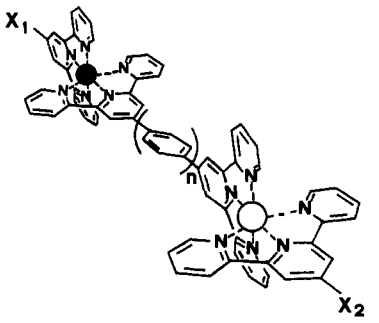

● Ru^{2+}
○ Os^{2+}

1 $X_1 = X_2 =$ ph Me, n = 0
2 $X_1 = X_2 =$ ph Me, n = 1
3 $X_1 = X_2 =$ ph Me, n = 2
4 $X_1 = SO_2Me$, $X_2 = H$, n = 0
5 $X_1 = SO_2Me$, $X_2 = H$, n = 1
6 $X_1 = SO_2Me$, $X_2 =$ ph Me, n = 2

Figure 1. Schematic structures of the dinuclear compounds.

Experimental Section

Preparation of the Compounds. **[(Meph-tpy)Ru(tpy-tpy)]$(PF_6)_2$.** Ru(Meph-tpy)Cl_3[11] (110 mg, 0.21 mmol) and $AgBF_4$ (125 mg, 0.64 mmol) were refluxed in air for 2 h in acetone (50 mL). The reaction mixture was filtered to remove AgCl, DMF (100 mL) was added, and the acetone was evaporated. The resulting solution was slowly added under argon to a hot solution (80 °C) of the ligand tpy-tpy (144 mg, 0.31 mmol) in DMF (100 mL). The mixture was refluxed under argon for 1 h. DMF was then evaporated under reduced pressure, and acetonitrile (150 mL) and KPF_6 (400 mg) were added. The hexafluorophosphate salts of the complexes were precipitated by addition of water (150 mL) and evaporation of acetonitrile. The precipitate obtained was washed with water (2 × 50 mL) and ether (2 × 50 mL) and subjected to a silica gel column chromatography (eluent acetonitrile) to give 208 mg of pure complex (yield, 85%). ^1H NMR (200 MHz, DMSO-d_6): δ 9.67 (2H, s); 9.48 (2H, s); 9.26 (2H, s); 9.23 (2H, d, 8.2 Hz); 9.13 (2H, d, 8.0 Hz); 8.87 (2H, d, 4.0 Hz); 8.82 (2H, d, 7.6 Hz); 8.39 (2H, d, 8.3 Hz); 8.15 (2H, ddd, 7.8, 7.8, 1.7 Hz); 8.07 (4H, m); 7.62 (8H, m); 7.30 (4H, m).

[(Meph-tpy)Ru(tpy-ph-tpy)]$(PF_6)_2$. The same procedure as above was used (yield, 77%). ^1H NMR (200 MHz, CD_3CN): δ 9.08 (2H, s); 8.99 (2H, s); 8.91 (2H, s); 8.71 (8H, m), 8.41 (2H, d, 8.3 Hz); 8.26 (2H, d, 8.3 Hz); 8.11 (2H, d, 8.0 Hz); 7.97 (6H, ddd, 15.4, 7.6, 1.8 Hz); 7.58 (2H, d, 8.0 Hz); 7.48 (6H, m); 7.20 (4H, dd, 7.3, 5.9 Hz); 2.55 (3H, s).

[(Meph-tpy)Ru(tpy(ph)$_2$tpy)]$(PF_6)_2$. The same experimental procedure as [(Meph-tpy)Ru(tpy-tpy)]$[PF_6)_2$ was used (yield, 76%). ^1H NMR (200 MHz, CD_3CN): δ 9.09 (2H, s); 9.00 (2H, s); 8.87 (2H, s); 8.71 (8H, m); 8.37 (2H, d, 8.6 Hz); 8.16 (2H, d, 8.8 Hz); 8.10, (6H, m); 7.96 (6H, m); 7.59 (2H, d, 8.3 Hz); 7.48 (6H, m); 7.19 (4H, dd, 6.4, 6.4 Hz); 2.55 (3H, s).

[(MeO_2S-tpy)Ru(tpy(ph)$_2$tpy)]$(PF_6)_2$. The same experimental procedure as [(Meph-tpy)Ru(tpy-tpy)]$(PF_6)_2$ was used (yield, 60%). ^1H NMR (200 MHz, CD_3CN): δ 9.15 (2H, s); 9.10 (2H, s); 8.87 (2H, s); 8.77 (8H, m); 8.38 (2H, d, 8.4 Hz); 8.19 (6H, m); 7.98 (4H, m); 7.69 (2H, m); 7.54 (2H, d, 5.0 Hz); 7.32 (6H, m); 7.17 (2H, m); 3.53 (3H, s).

[(Meph-tpy)Ru(tpy-tpy)Os(tpy-phMe)]$(PF_6)_4$ (1). [(Meph-tpy)Ru(tpy-tpy)]$(PF_6)_2$ (67 mg, 0.056 mmol) and (Meph-tpy)$OsCl_3$ (35 mg, 0.056 mmol) were refluxed under argon in butanol (50 mL) for 7 h. After removing the solvent, acetonitrile (100 mL) and KPF_6 (200 mg) were added. The hexafluorophosphate salts were precipitated by addition of water (150 mL) and evaporation of acetonitrile. The precipitate was washed with water (2 × 50 mL) and ether (2 × 50 mL) and subjected to silica gel chromatography (eluent, acetonitrile and 10% aqueous KNO_3 0.4 M) to give 26 mg of complex **1** (yield, 23%) and a by-product (Meph-tpy)Ru(tpy-tpy)$OsCl_3(PF_6)_2$ (yield, 12%), which was characterized by FAB-MS (nitrobenzyl alcohol matrix); m/z = 1331.0; [(Meph-tpy)-Ru(tpy-tpy)$OsCl_3(PF_6)$]$^+$ requires 1331.0.

^1H NMR (400 MHz, DMSO-d_6): δ 9.91 (2H, s); 9.89 (2H, s); 9.56 (2H, s); 9.52 (2H, s); 9.18 (8H, m); 8.40 (2H, d, 4.1 Hz); 8.36 (2H, d,

4.1 Hz); 8.23 (2H, m); 8.10 (4H, m); 7.99 (2H, m); 7.70 (2H, d, 2.9 Hz); 7.61 (6H, m); 7.53 (2H, d, 2.4 Hz); 7.38 (8H, m); 7.28 (2H, m); 2.58 (3H, s); 2.55 (3H, s). FAB-MS (nitrobenzyl alcohol matrix): m/z = 1839.0; [(Meph-tpy)Ru(tpy-tpy)Os(tpy-phMe)$(PF_6)_3$]$^+$ requires 1839.2.

[Meph-tpy)Ru(tpy-ph-tpy)Os(tpy-phMe)][PF_6]$_4$ (2). This compound was prepared in an analogous way to **1** (yield, 32%). ^{1}H NMR (200 MHz, CD_3CN): δ 9.19 (2H, s); 9.17 (2H, s); 9.05 (2H, s); 9.03 (2H, s); 8.70 (8H, m); 8.58 (4H, s); 8.14 (2H, d, 7.7 Hz); 8.10 (2H, d, 7.8 Hz); 7.99 (4H, m); 7.85 (4H, m); 7.60 (4H, d, 8.3 Hz); 7.48 (4H, d, 5.3 Hz); 7.37 (2H, d, 5.1 Hz); 7.34 (2H, d, 5.1 Hz); 7.17 (8H, m), 2.59 (3H, s); 2.56 (3H, s). FAB-MS (nitrobenzyl alcohol matrix): m/z = 1915.2; [(Meph-tpy)Ru(tpy-ph-tpy)Os(tpy-phMe)$(PF_6)_3$]$^+$ requires 1915.2.

The side product [(Meph-tpy)Ru(tpy-ph-tpy)$OsCl_3$]$(PF_6)_2$ was also isolated in 10% yield. FAB-MS (nitrobenzyl alcohol matrix): m/z = 1406.5; [(Meph-tpy)Ru(tpy-ph-tpy)$OsCl_3(PF_6)$]$^+$ requires 1407.0.

The trinuclear complex [(Meph-tpy)Ru(tpy-ph-tpy)Os(tpy-ph-tpy)-Ru(tpy-phMe)]$(PF_6)_6$ was obtained as a third fraction in the course of the chromatographic separation (yield, 10%). ^{1}H NMR (200 MHz, CD_3CN): δ 9.25 (4H, s); 9.20 (4H, s); 9.04 (4H, s); 9.31 (8H, d, 8.1 Hz); 9.21 (4H, d, 8.2 Hz); 9.14 (8H, s); 8.67 (4H, d, 8.2 Hz); 8.48 (12 H, m); 8.13 (4H, d, 8.2 Hz); 8.02 (8H, d, 4.9 Hz); 7.95 (4H, d, 5.5 Hz); 7.77 (12H, m). FAB-MS (nitrobenzyl alcohol matrix): m/z = 2843.8; [(Meph-tpy)Ru(tpy-ph-tpy)Os(tpy-ph-tpy)Ru(tpy-phMe)$(PF_6)_5$]$^+$ requires 2845.2.

[(Meph-tpy)Ru(tpy(ph)$_2$tpy)Os(tpy-phMe)][PF_6]$_4$ (3). The same experimental procedure as for **1** and **2** was used (yield, 15%). ^{1}H NMR (400 MHz, DMSO-d_6): δ 9.58 (2H, s); 9.56 (2H, s); 9.49 (2H, s); 9.47 (2H, s); 9.12 (8H, m); 8.66 (2H, d, 4.0 Hz); 8.62 (2H, d, 4.0 Hz); 8.37 (4H, d, 4.0 Hz); 8.33 (4H, d, 4.0 Hz); 8.09 (4H, dd, 7.5, 3.7 Hz); 7.95 (4H, dd, 7.6, 3.8 Hz); 7.59 (8H, m); 7.46 (2H, d, 3.2 Hz); 7.45 (2H, d, 3.2 Hz); 7.32 (4H, m); 7.24 (4H, m); 2.57 (3H, s); 2.54 (3H, s). FAB-MS (nitrobenzyl alcohol matrix): m/z = 1991.3; [(Meph-tpy)Ru(tpy-(ph)$_2$tpy)Os(tpy-phMe)$(PF_6)_3$]$^+$ requires 1991.3. [(Meph-tpy)Ru(tpy-(ph)$_2$tpy)$OsCl_3$]$(PF_6)_2$ was obtained as a by-product in 15% yield. FAB-MS (nitrobenzyl alcohol matrix): m/z = 1482.9; [(Meph-tpy)Ru(tpy-(ph)$_2$tpy)$OsCl_3(PF_6)$]$^+$ requires 1483.1.

[MeO_2S-tpy)Ru(tpy-tpy)][PF_6]$_2$. A suspension of tpy-tpy (0.10 mmol) and [Ru($MeSO_2$tpy)Cl_3] (0.09 mmol) in 1,2-ethanediol (10 mL) was refluxed for 20 min. The red solution was allowed to cool, and 10 mL of water was added, along with an excess of methanolic [NH_4][PF_6]. The precipitate was collected by filtration and redissolved in the minimum volume of acetonitrile for column chromatography (silica; acetonitrile, saturated aqueous potassium nitrate, water (7:1:0.5 v/v) as eluent). The main orange product fraction was collected, and water (25 mL) and excess methanolic [NH_4][PF_6] were then added. The mixture was reduced in volume *in vacuo* to precipitate the complex as the hexafluorophosphate salt. Recrystallization from acetone–methanol or acetonitrile–water gave the complex as an analytically pure red powder in 20–40% yield. ^{1}H NMR (250 MHz, CD_3CN): δ 9.22 (2H, s); 9.20 (2H, s); 9.15 (2H, s); 8.85 (2H, d, 8.1 Hz); 8.82 (2H, d, 5.5 Hz); 8.69 (4H, d); 8.08 (2H, dd); 7.97 (4H, m); 7.55 (4H, m); 7.36 (2H, d, 5.5 Hz); 7.27 (2H, dd); 7.17 (2H, dd); 3.52 (3H, s). FAB-MS (nitrobenzyl alcohol matrix): m/z = 1023; [(MeO_2S-tpy)Ru(tpy-tpy)][PF_6]$^+$ requires 1022.

[(MeO_2S-tpy)Ru(tpy-ph-tpy)][PF_6]$_2$. A suspension of tpy-ph-tpy (0.120 g, 0.22 mmol) and [Ru(MeO_2Stpy)Cl_3] (0.110 g, 0.21 mmol) in 1,2-ethanediol (10 cm^3) was refluxed for 45 min and the red solution cooled. Water (10 mL) was added, along with an excess of methanolic [NH_4]-[PF_6], and the precipitate was redissolved in the minimum volume of acetonitrile for column chromatography on silica (column 15 cm long, 3 cm wide; acetonitrile, saturated aqueous potassium nitrate, water (7:1:0.5 v/v) as eluent). The main orange product fraction was collected, and water (25 mL) and excess methanolic [NH_4][PF_6] were added. The mixture was reduced in volume *in vacuo* to precipitate the complex as the hexafluorophosphate salt. Recrystallization from 1:1 acetone–methanol gave [(MeO_2Stpy)Ru(tpy-ph-tpy)][PF_6]$_2$ as an analytically pure brown powder (0.065 g, 22%). ^{1}H NMR (250 MHz, CD_3CN): δ 9.14 (2H, s); 9.11 (2H, s); 8.94 (2H, s); 8.77 (4H, m); 8.69 (4H, d, 7.9 Hz); 8.42 (2H, ABd, 8.3 Hz); 8.31 (2H, ABd, 8.3 Hz); 7.99 (6H, m); 7.52 (4H, m); 7.36 (2H, d, 5.3 Hz); 7.28 (2H, dd); 7.16 (2H, dd); 3.51 (3H, s). FAB-MS (nitrobenzyl alcohol matrix: m/z = 1023; [(MeO_2S-tpy)Ru(tpy-tpy)][PF_6]$^+$ requires 1022.

[(MeO_2S-tpy)Ru(tpy-tpy)Os(tpy)][PF_6]$_4$ (4). A suspension of Os(tpy)Cl_3 (21 mg, 0.04 mmol) and [(MeO_2S-tpy)Ru(tpy-tpy)][PF_6]$_2$ (45 mg, 0.04 mmol) in 1,2-ethanediol (10 mL) was refluxed for 1 h. The purple-brown solution was cooled, and water (10 mL) and an excess of methanolic NH_4PF_6 were added. The precipitated hexafluorophosphate salts were dissolved in the minimum volume of acetonitrile and chromatographed on silica (acetonitrile, saturated aqueous potassium nitrate, water (7:1:0.5 v/v) as eluent) to give 13 mg of pure complex (yield, 18%). ^{1}H NMR (250 MHz, CD_3CN): δ 9.46 (2H, s); 9.45 (2H, s); 9.19 (2H, s); 8.85 (6H, m); 8.74 (2H, d, 7.8 Hz); 8.52 (2H, d, 8.25 Hz); 8.05 (5H, m); 7.93 (2H, t, 8.2 Hz); 7.82 (2H, t, 7.8 Hz); 7.57 (2H, d, 5.5 Hz); 7.44 (2H, d, 5.5 Hz); 7.35 (4H, m); 7.25 (8H, m); 3.55 (3H, s). FAB-MS (nitrobenzyl alcohol matrix): m/z = 1099; [(MeO_2S-tpy)Ru(tpy-tpy)Os(tpy)][PF_6]$_3^+$ requires 1098.

[(MeO_2S-tpy)Ru(tpy-ph-tpy)Os(tpy)][PF_6]$_4$ (5). This was prepared in an analogous way to **4** (yield, 15%). ^{1}H NMR (250 MHz, CD_3CN): δ 9.18 (6H, s); 8.80 (2H, d, 8.25 Hz); 8.73 (6H, m); 8.57 (4H, m, AB); 8.51 (2H, d, 8 Hz); 8.0 (5H, m); 7.86 (2H, t); 7.81 (2H, t); 7.56 (2H, d, 5.5 Hz); 7.39 (2H, d, 5.8 Hz); 7.30 (6H, m); 7.16 (6H, m); 3.53 (3H, s). FAB-MS (nitrobenzyl alcohol matrix): m/z = 1812; [(MeO_2S-tpy)Ru(tpy-ph-tpy)Os(tpy)][PF_6]$_3^+$ requires 1813.

[(MeO_2S-tpy)Ru(tpy(ph)$_2$tpy)Os(tpy-phMe)][PF_6]$_4$ (6). The same procedure as for **1** was used (yield, 10%). ^{1}H NMR (200 MHz, DMSO-d_6): δ 9.62 (4H, s); 9.54 (2H, s); 9.52 (2H, s); 9.16 (8H, m); 8.68 (2H, d, 8.1 Hz); 8.64 (2H, d, 8.5 Hz); 8.36 (6H, d, 8.3 Hz); 8.12 (4H, m); 7.96 (4H, m); 7.67 (2H, d, 5.6 Hz); 7.47 (12H, m); 7.26 (4H, m); 3.73 (3H, s). FAB-MS (nitrobenzyl alcohol matrix) m/z = 1978.4; [(MeO_2S-tpy)Ru(tpy(ph)$_2$tpy)Os(tpy-phMe)$(PF_6)_3$]$^+$ requires 1979.2.

Equipment. The instruments and procedure used to obtain cyclic voltammograms (acetonitrile/n-Bu_4NBF_4 0.1 M)[11,19] and absorption spectra[11] have been described in previous papers. Uncorrected luminescence spectra of deaerated solutions ($\leq 1.0 \times 10^{-5}$ M) were obtained with a Spex Fluorolog II spectrofluorimeter. Luminescence quantum yields were computed by using corrected spectra, obtained by employing software provided by the firm, and using Os(tpy)$_3^{2+}$ as a standard (Φ = 0.005).[20] Time-resolved luminescence experiments were performed either with an IBH single photon counting equipment or with a picosecond fluorescence spectrometer based on a Nd:YAG (PY62-10 Continuum) laser and a Hamamatsu C1587 streak camera.[21] The estimated errors are 10% on quantum yields and 8% and 20% on nanosecond and picosecond lifetimes, respectively.

Results and Discussion

Synthesis of the Complexes. The ligands Meph-tpy (4′-(*p*-tolyl)-2,2′:6′,2″-terpyridine),[11] MeO_2S-tpy (4′-(2,2′:6′,2″-terpyridinyl)methyl sulfone),[13] tpy-tpy,[9,22] tpy-ph-tpy,[23] and tpy-(ph)$_2$tpy[24] have been synthesized as described previously.

Ru(tpy-phMe)$_2^{2+}$ and Os(tpy-phMe)$_2^{2+}$ have been synthesized following literature methods.[8,11]

The general preparation of the ruthenium–osmium dinuclear complexes is given in Scheme 2. The key complexes (Meph-tpy)Ru(tpy(ph)$_n$tpy)$^{2+}$ for the synthesis of heterodinuclear compounds can be obtained by reaction of a labile solvated ruthenium precursor (Meph-tpy)Ru(acetone)$_3^{2+}$ with an excess of bridging ligand. In a second step the ruthenium complex bearing a free terpyridine site is allowed to react with (Meph-tpy)$OsCl_3$. This very insoluble compound is used without further purification. In fact, attempts to remove the chloride ions with Ag^+ were inconclusive. Depending upon the starting sample, two other ruthenium–osmium complexes could be isolated in low yield: a dinuclear compound where the Os atom was coordinated to three Cl atoms and a trinuclear complex (Scheme 3). Their formation seems to indicate the polymeric nature of the poorly defined starting complex of (Meph-tpy)$OsCl_3$.

(19) Constable, E. C.; Cargill Thompson, A. M. W.; Tocher, D. A.; Daniels, M. A. M. *New J. Chem.* **1992**, *16*, 855.
(20) Kober, E.; Caspar, J. V.; Lumpkin, R. S.; Meyer, T. J. *J. Phys. Chem.* **1986**, *90*, 3722.
(21) Armaroli, N.; Balzani, V.; Barigelletti, F.; De Cola, L.; Flamigni, L.; Sauvage, J.-P.; Hemmert, C. *J. Am. Chem. Soc.*, in press.
(22) Constable, E. C.; Ward, M. D. *J. Chem. Soc., Dalton Trans.* **1990**, 1405.
(23) Kröhnke, F. *Synthesis* **1976**, 1.
(24) (a) Collin, J.-P.; Lainé, P.; Launay, J.-P.; Sauvage, J.-P.; Sour, A. *J. Chem. Soc., Chem. Commun.* **1993**, 434. (b) Constable, E. C.; Cargill Thompson, A. M. W.; Tocher, D. A. *Polym. Prepr. (Am. Chem. Soc., Div. Polym. Chem.)* **1993**, *34*, 110. (c) Constable, E. C.; Cargill Thompson, A. M. W.; Tocher, D. A. *Makromol. Chem.*, in press.

Scheme 2

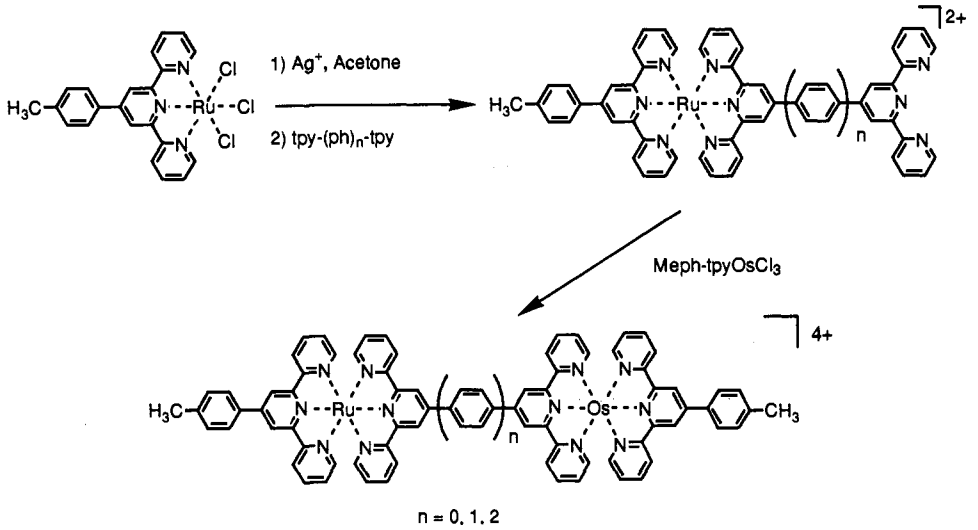

Scheme 3

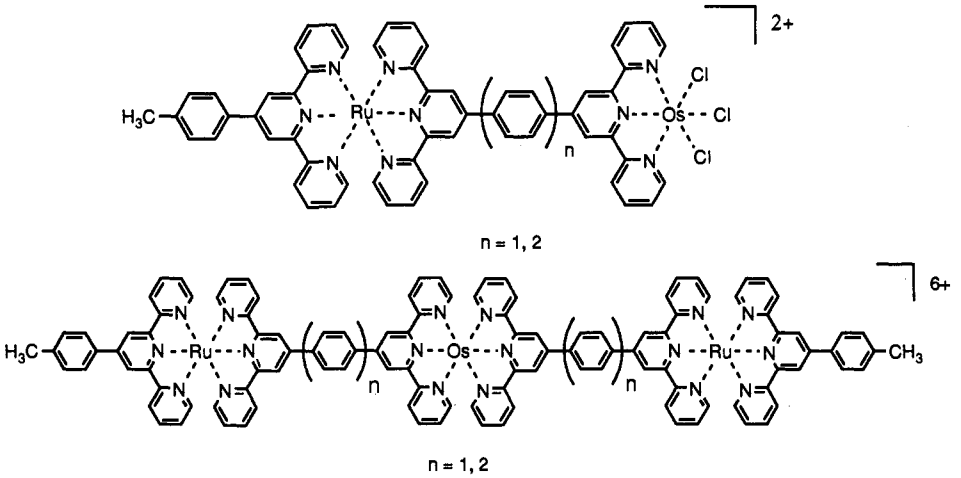

Table 1. Absorption Spectra[a]

	λ_{max}, nm (ϵ, M^{-1} cm^{-1})			
	ligand centered		^{1}MLCT	^{3}MLCT
$Ru(tpy)_2^{2+}$ [b]	270(31 600)	307(52 400)	475(11 600)	
$Ru(tpy\text{-}phMe)_2^{2+}$ [c]	284(68 000)	310(75 800)	490(29 300)	
$Ru(tpy\text{-}SO_2Me)_2^{2+}$ [d]	274(42 900)	313(45 900)	486(20 200)	
$Os(tpy)_2^{2+}$ [b]	270(43 900)	310(74 200)	475(15 400)	656(4200)
$Os(tpy\text{-}phMe)_2^{2+}$ [e]	286(58 000)	314(68 000)	490(26 000)	667(6600)
1, (Meph-tpy)Ru(tpy-tpy)Os(tpy-phMe)$^{4+}$	288(130 000)	312(133 000)	522(62 100)	678(10 500)
2, (Meph-tpy)Ru(tpy-ph-tpy)Os(tpy-phMe)$^{4+}$	288(113 000)	312(137 000)	500(65 600)	671(8500)
3, (Meph-tpy)Ru(tpy(ph)$_2$tpy)Os(tpy-phMe)$^{4+}$	284(112 700)	314(139 000)	496(66 100)	670(7700)
4, (MeO_2S-tpy)Ru(tpy-tpy)Os(tpy)$^{4+}$	275(69 700)	310(838 00)	515(40 600)	672(6500)
5, (MeO_2S-tpy)Ru(tpy-ph-tpy)Os(tpy)$^{4+}$	275(73 500)	310(116 000)	496(53 700)	665(6200)
6, (MeO_2S-tpy)Ru(tpy(ph)$_2$tpy)Os(tpy-phMe)$^{4+}$	275(79 200)	315(116 000)	495(55 700)	670(4200)

[a] Acetonitrile solution, room temperature. [b] Constable, E. C.; Cargill Thompson, A. M. W. *J. Chem. Soc., Dalton Trans.*, in press. [c] Reference 11. [d] Reference 13. [e] Reference 12.

The six novel dinuclear compounds can be grouped into two families. The first one (**1–3**) contains (Meph-tpy)Ru^{2+} and Os(tpy-phMe)$^{2+}$ units connected by tpy(ph)$_n$tpy (n = 0, 1, 2) bridging ligands. The second family (**4–6**) differs from the first one for two reasons: (i) in the Ru moiety, the Meph substituent on the 4′ position of the external tpy ligand has been replaced by the strong π electron acceptor MeO_2S group; (ii) in **4** and **5**, in the Os moiety the Meph substituent on the 4′ position of the external tpy ligand has been replaced by hydrogen (in **6**, the Os moiety has not been varied). Comparison of the results obtained for complexes of the same family allows us to discuss the problem of electronic interaction through the different bridges. Comparison of the results obtained for members of the two families which contain the same bridging ligand can yield information on the change in the intercomponent interaction on changing the substituents on the external tpy ligands.

Most of the results obtained are collected in Tables 1–3, where some relevant data for mononuclear reference compounds are also displayed for comparison purposes.

Absorption Spectra. The visible parts of the absorption spectra of the novel dinuclear compounds **4**, **5**, and **6** are shown in Figure 2, and the absorption maxima of all the complexes and of some reference compounds are collected in Table 1. The absorption spectra of the dinuclear species of the same family are considerably

Table 2. Electrochemical Results[a]

	E_{ox}^{II}(Ru)	E_{ox}^{I}(Os)	E_{red}^{I}	E_{red}^{II}
$Ru(tpy)_2^{2+}$ [b]	+1.30		−1.29	−1.54
$Ru(tpy\text{-}phMe)_2^{2+}$ [c]	+1.25		−1.24	−1.46
$Ru(tpy\text{-}SO_2Me)_2^{2+}$ [d]	+1.48		−0.96	−1.23
$Os(tpy)_2^{2+}$ [b]		+0.96	−1.25	−1.57
$Os(tpy\text{-}phMe)_2^{2+}$ [e]		+0.93	−1.23	−1.54
1, (Meph-tpy)Ru(tpy-tpy)Os(tpy-phMe)$^{4+}$	+1.27(60)	+0.90(60)	−1.01(70)	−1.28(60)
2, (Meph-tpy)Ru(tpy-ph-tpy)Os(tpy-phMe)$^{4+}$	+1.25(60)	+0.90(60)	−1.20(100)[g]	−1.43(120)[f]
3, (Meph-tpy)Ru(tpy(ph)$_2$tpy)Os(tpy-phMe)$^{4+}$	+1.24(70)	+0.90(60)	−1.22(80)[g]	−1.44(100)[f]
4, (MeO_2S-tpy)Ru(tpy-tpy)Os(tpy)$^{4+}$	+1.44(105)	+0.99(110)	−0.95(90)	−1.09(90)
5, (MeO_2S-tpy)Ru(tpy-ph-tpy)Os(tpy)$^{4+}$	+1.39(105)	+0.94(110)	−1.01(75)	−1.17(100)
6, (MeO_2S-tpy)Ru(tpy(ph)$_2$tpy)Os(tpy-phMe)$^{4+}$	+1.31(60)	+0.90(60)	−1.00(60)	−1.20(60)[g]

[a] Acetonitrile solution, 0.1 M Bu_4NBF_4, room temperature; potentials in V, *vs* SCE; the literature data in V *vs* Fc^+/Fc have been converted by adding 0.38 V; the values in parentheses are the differences between the anodic and cathodic peaks of the CV waves. [b] Constable, E. C.; Cargill Thompson, A. M. W. *J. Chem. Soc., Dalton Trans.*, in press. [c] Reference 12. [d] Reference 13. [e] Beley, M.; Collin, J. P.; Sauvage, J. P.; Sugihara, H.; Heisel, F.; Miehé, A. *J. Chem. Soc., Dalton Trans.* **1991**, 3157. [f] Two-electron wave. [g] This one-electron wave is followed by a two-electron wave at −1.42 V (100).

Table 3. Luminescence Data[a]

	293 K						77 K			
	Ru-based		Os-based				Ru-based		Os-based	
	$\bar{\nu}_{max}$, cm^{-1}	τ, ns	$\bar{\nu}_{max}$, cm^{-1}	τ, ns	I_{rel}[b] (500 nm)	I_{rel}[c] (650 nm)	$\bar{\nu}_{max}$, cm^{-1}	τ, μs	$\bar{\nu}_{max}$, cm^{-1}	τ, μs
$Ru(tpy)_2^{2+}$ [d]	e	0.25					16 725	11		
$Ru(Meph\text{-}tpy)_2^{2+}$ [d]	15 625	0.95[f]					15 925	9.1		
$Ru(MeO_2S\text{-}tpy)_2^{2+}$ [f]	15 375	25[h]					15 825	10.5		
$Os(tpy)_2^{2+}$ [d]			13 925	269					14 525	3.9
$Os(Meph\text{-}tpy)_2^{2+}$ [d]			13 625	230	100	100			13 800	2.8
1, (Meph-tpy)Ru(tpy-tpy)Os(tpy-phMe)$^{4+}$	e	i	12 500	110	6	7	e	i	13 275	1.8
2, (Meph-tpy)Ru(tpy-ph-tpy)Os(tpy-phMe)$^{4+}$	e	i	13 400	190	71	70	e	i	13 775	2.8
3, (Meph-tpy)Ru(tpy(ph)$_2$tpy)Os(tpy-phMe)$^{4+}$	e	i	13 550	200	72	61	e	i	13 800	2.8
4, (MeO_2S-tpy)Ru(tpy-tpy)Os(tpy)$^{4+}$	e	i	12 600	130	7	7	e	i	13 200	1.6
5, (MeO_2S-tpy)Ru(tpy-ph-tpy)Os(tpy)$^{4+}$	e	i	13 475	213	54	60	e	i	13 775	2.7
6, (MeO_2S-tpy)Ru(tpy(ph)$_2$tpy)Os(tpy-phMe)$^{4+}$	e	i	13 550	219	67	74	e	i	13 725	2.6

[a] Deaerated butyronitrile solutions. [b] Relative luminescence intensity with λ_{exc} = 500 nm. At this excitation wavelength the Ru-based and Os-based units of the dinuclear complexes are excited in an approximately 1:1 ratio (see Figures 2 and 3). [c] Relative luminescence intensity with λ_{exc} = 650 nm. At this excitation wavelength only the Os-based units of the dinuclear complexes are excited. [d] Reference 10. [e] No band maximum observed in the region of the expected Ru-based emission. [f] $\Phi_{em} = 3.2 \times 10^{-5}$, ref 15a. [g] Reference 13. [h] $\Phi_{em} = 4.0 \times 10^{-4}$, ref 13a. [i] Only the picosecond excitation pulse is registered.

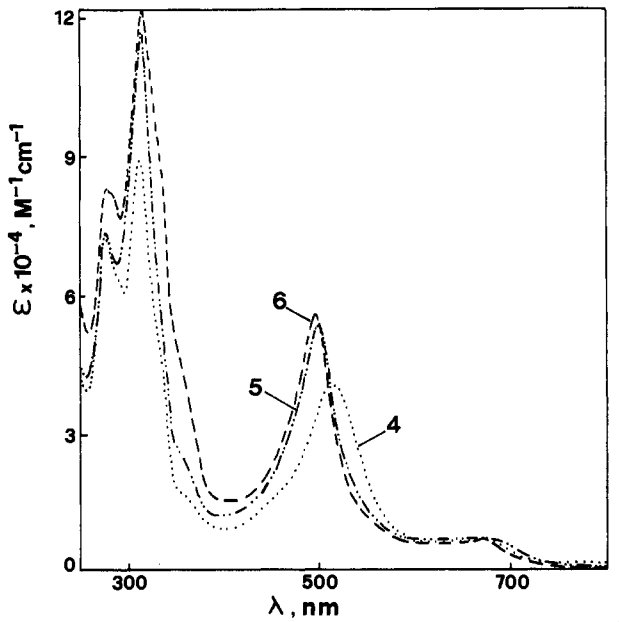

Figure 2. Absorption spectra (room temperature, butyronitrile solution) of (MeO_2S-tpy)Ru(tpy-tpy)Os(tpy)$^{4+}$ (**4**), (MeO_2S-tpy)Ru(tpy-ph-tpy)-Os(tpy)$^{4+}$ (**5**), and (MeO_2S-tpy)Ru(tpy(ph)$_2$tpy)Os(tpy-phMe)$^{4+}$ (**6**).

different in the visible region, even though the spacers do not absorb in that region. For both families, the bands in the visible region are metal-to-ligand charge-transfer (MLCT) in character.[15] They move to lower energy as the metal–metal separation distance decreases. A comparison with the available data for the mononuclear components (Table 1) can help in understanding the reason for this trend. For example, in the $M(tpy)_2^{2+}$ and $M(tpy\text{-}phMe)_2^{2+}$ reference compounds the value of λ_{max} of the ^{1}MLCT band does not depend on whether M is Ru or Os, whereas for the complexes of the same metal the Meph substituent displaces λ_{max} to lower energy. In compound **3**, which is made of Ru and Os units very similar to the $M(tpy\text{-}phMe)_2^{2+}$ reference compounds, λ_{max} is shifted to lower energy compared with $M(tpy\text{-}phMe)_2^{2+}$. On passing to **2** and **1**, λ_{max} moves further to the red. This behavior suggests that the acceptor orbital of the MLCT transition is located on the tpy ligands belonging to the bridge, as will be clearly shown by the electrochemical results (*vide infra*).

Electrochemical Behavior. The electrochemical results obtained for the six novel dinuclear compounds are gathered in Table 2 together with the results available for the reference mononuclear species. Several interesting correlations emerge from the examination of this set of data. Concerning the mononuclear compounds, one can notice that (i) Ru is oxidized at much more positive potentials than Os; (ii) the ligands are reduced at similar potentials in the Ru and Os compounds; (iii) the Meph substituent moves the oxidation potential to slightly less positive values and the reduction potential to slightly less negative values; and (iv) the MeO_2S substituent makes the oxidation potential much more positive and the reduction potential much less negative.

Compound **1** shows two reversible oxidation waves, which can be straightforwardly assigned to the Os-based (+0.94 V) and Ru-based (+1.31 V) moieties. The oxidation potential of the Os-based moiety is practically the average of the oxidation potentials of the $Os(tpy)_2^{2+}$ and $Os(Meph\text{-}tpy)_2^{2+}$ model compounds. For the Ru-based moiety, the oxidation potential is slightly higher than those of the corresponding model compounds, as expected because of the electron acceptor properties of the already oxidized (3+ charge) Os-based moiety. As one can see

from Table 2, the first reduction potential of **1** is much less negative than the first reduction potential of the parent compounds. This indicates that the LUMO orbital of the dinuclear complex is located on the bridging ligand where the two tpy units interact strongly, as is also shown by the absorption spectra (*vide supra*). The second reduction potential is very close to the *first* reduction potential of the parent compounds. This would indicate that either the second reduction process of **1** concerns again the bridge or the monoreduced bridge does not affect the reduction of an external Meph-tpy ligand. In the second case, however, independent simultaneous reduction of the two external ligands would be expected.

When one or two phenylene spacers are interposed between the Ru-based and Os-based units, the oxidation potential of the Os-based moiety is not affected. The small decrease of the oxidation potential of the Ru-based moiety may reflect the decrease of the electron acceptor effect of the already oxidized Os-based moiety with increasing distance. The effect of the ph spacers is much more dramatic on the reduction potentials. In **2** the first reduction wave occurs at a potential more negative than that of **1**, but still slightly more positive than that of the parent compounds. It seems likely, therefore, that the first reduction process again involves the bridging ligand. The big difference with respect to **1** is that in **2** the two tpy moieties of the bridging ligand do not interact strongly with each other because of the presence of the phenylene spacer, so that the LUMO of the two inner ligands lies at energies much closer to that of the external ligands. Another important difference is that in **2** the first reduction wave involves two electrons. In other words, the second reduction process in **2** occurs at a potential almost coincident to that of the first one and less negative than the second reduction process of **1**. This would exclude the possibility that the first and second reduction processes of **2** concern the two moieties of the bridging ligand or the two ligands of the same metal-based unit. In order to reduce electron repulsion, in fact, the two-electron-reduced species of **2** should correspond to the one-electron reduction of a bridging ph-tpy unit and of an external Meph-tpy ligand, coordinated to different metal centers. Further reduction of **2** (Table 2) involves again two electrons at almost the same potential. This means that such processes involve uncoupled sites, i.e. ligands units not directly linked and belonging to different metals, in agreement with the above discussion on the first two reduction processes.

In compound **3** the Ru-based and Os-based oxidation potentials are very close to those of **2** (and **1**), showing that interposition of another ph spacer does not substantially affect the metal–metal interaction that, as well have seen above, is already small in **1**. As far as reduction is concerned, one can notice again two well-separated waves, each corresponding to two almost equivalent sites. Therefore, the two observed waves should not correspond to inner–inner and outer–outer ligand couples, but rather to two inner–outer ligand couples, in agreement with the conclusion drawn above for **2**.

The oxidation potential of the Os-based moiety of **4** is slightly more positive than that of the $Os(tpy)_2^{2+}$ model compound, contrary to what happens for **1** (*vide supra*). This is likely to be related to the presence of the strongly electron-withdrawing MeO_2S substituent on the outer tpy ligand of the Ru-based moiety. The oxidation potential of the Ru-based moiety of **4** is much more positive than the average of the oxidation potentials of the $Ru(tpy)_2^{2+}$ and $Ru(tpy\text{-}SO_2Me)_2^{2+}$ model compounds because of the electron-withdrawing effect of the already oxidized Os-based moiety. Interestingly, the first oxidation potential of the model symmetrical dinuclear compound $(MeO_2S\text{-}tpy)Ru(tpy\text{-}tpy)Ru(tpy\text{-}SO_2Me)^{4+}$ (+1.45 V)[9] is very close to that of the Ru-based moiety of **4** (i.e., to its second oxidation potential), indicating that the $Os(tpy)^{3+}$ and $Ru(tpy\text{-}SO_2Me)^{2+}$ "terminator" units show very similar electronic effects.

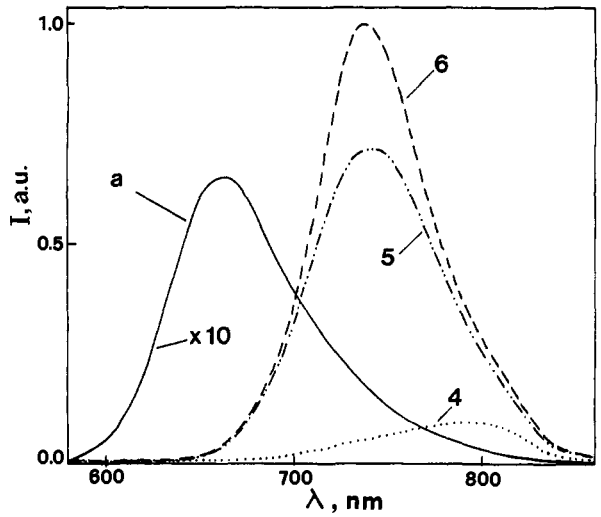

Figure 3. Luminescence spectra (room temperature, isoabsorptive butyronitrile solutions, λ_{exc} 500 nm) of $(MeO_2S\text{-}tpy)Ru(tpy\text{-}tpy)Os(tpy)^{4+}$ (**4**), $(MeO_2S\text{-}tpy)Ru(tpy\text{-}ph\text{-}tpy)Os(tpy)^{4+}$ (**5**), $(MeO_2S\text{-}tpy)Ru(tpy(ph)_2\text{-}tpy)Os(tpy\text{-}phMe)^{4+}$ (**6**), and the reference compound $Ru(tpy\text{-}SO_2Me)_2^{2+}$ (curve a).

The first oxidation potential of **5** is less positive than that of **4** because of the smaller interaction with the Ru-based electron acceptor moiety. The decrease in the oxidation potential of the Ru-based moiety is to be attributed to the smaller electron-withdrawing effect of the already oxidized Os-based moiety (again, the first oxidation potential of the symmetric dinuclear Ru compound is identical to that of the Ru-based moiety of **5**). Insertion of another ph spacer (compound **6**) would be expected to have a smaller effect, but it must also be considered that in going from **4** and **5** to **6** a Meph-tpy substituent has been placed on the outer tpy ligand of Os.

The first reduction potential of **4** is slightly less negative than that of **1** (where, as we have seen above, reduction takes place on the bridge) and very close to the first reduction potential of $Ru(MeO_2S\text{-}tpy)_2^{2+}$. Therefore, it is difficult to say whether the first reduction process takes place in the bridge or in the outer ligand of Ru. The second reduction process is much closer to the first on than in **1**. Therefore, it can be concluded that in the two-electron-reduced species the two reduced sites are the outer Ru ligand and the inner ligand on the Os side. The first reduction process of **5** can straightforwardly be assigned to the outer ligand of Ru, and the second one to the inner ligand of Os. The same assignment can be done for **6**. The first reduction process, in fact, occurs at almost the same potential in **5** and **6**, suggesting that it does not concern the bridge (compare with the behavior of **1**–**3**), and the second reduction potential becomes more negative in going from **5** to **6**, while the reverse would be expected for reduction on the outer ligand of Os.

Luminescence Properties. All the data concerning the luminescence behavior of the dinuclear complexes and of the reference compounds are collected in Table 3. The emission spectra at room temperature of compounds **4**–**6** are shown in Figure 3 together with the spectrum of $Ru(MeO_2S\text{-}tpy)_2^{2+}$.

All the Ru reference compounds exhibit a strong and long-lived luminescence at 77 K, and the Ru complexes bearing Meph or MeO_2S substituents in the 4′ position exhibit luminescence also at room temperature. In no case, however, is Ru-based luminescence observed for the dinuclear compounds (see, for example, Figures 3 and 4), because of quenching processes whose nature will be discussed in the next section. Given the instrumental characteristics of our equipment, we estimate that the lifetime of the Ru-based unit is $\leq$20 ps.[15] The present discussion will therefore concern the Os-based luminescence of the dinuclear compounds, for which the following correlations can be observed.

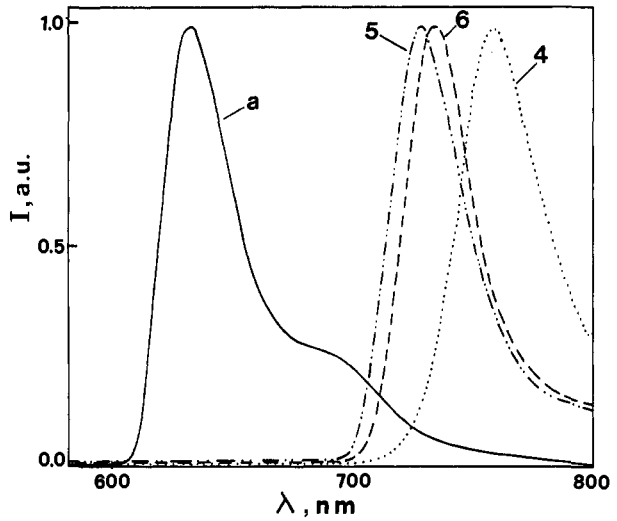

Figure 4. Normalized luminescence spectra (λ_{exc} 500 nm) at 77 K in butyronitrile rigid matrix of $(MeO_2S\text{-tpy})Ru(tpy\text{-}tpy)Os(tpy)^{4+}$ (**4**), $(MeO_2S\text{-tpy})Ru(tpy\text{-}ph\text{-}tpy)Os(tpy)^{4+}$ (**5**), $(MeO_2S\text{-tpy})Ru(tpy(ph)_2\text{-}tpy)Os(tpy\text{-}pHMe)^{4+}$ (**6**), and the reference compound $Ru(tpy\text{-}SO_2\text{-}Me)_2^{2+}$ (curve a).

(i) For **1** and **4**, the luminescence band is substantially red shifted compared to that of the $Os(tpy)_2^{2+}$ and $Os(Meph\text{-}tpy)_2^{2+}$ reference compounds. This shows that the lowest excited state of **1** and **4** involves a CT transition from Os(II) to the tpy-tpy bridging ligand, in agreement with the electrochemical results.

(ii) In going from **1** to **2** and **3**, and from **4** to **5** and **6**, the luminescence band moves to higher energies, but does not reach the energy of the Os(II) model compounds. This suggests that the lowest excited state concerns the bridging ligand in all the dinuclear compounds.

(iii) In all cases there is a blue shift in going from fluid solution to rigid matrix. This expected behavior for CT excited states is due to the lack of solvent repolarization in rigid matrix.[7] This effect should increase with increasing change in the dipole moment caused by the CT transition. In **1** and **4** the blue shift is much larger than in the reference compounds, which is consistent with the expected larger variation in the dipole moment when the CT transition involves the tpy-tpy bridging ligand. As expected, the blue shift decreases when the interaction between the two halves of the bridging ligand decreases because of the introduction of one or two ph spacers.

(iv) The emission bands of **1** and **2** at room temperature are red shifted with respect to those of **4** and **5**, respectively, as expected from the electrochemical data.

(v) The electrochemical data show that for **6** the site easier to oxidize (i.e., Os) is far away from the site easier to reduce (i.e., the outer MeO_2S-tpy ligand of Ru). This would suggest that the lowest excited state of **6** corresponds to a "remote" MLCT transition. This, however, does not seem to be the case since the luminescence behavior of **6** is exactly the same as that of **3**, where low-energy "remote" MLCT transitions are not present and Os is coordinated to the same ligands as in **6**. It should be recalled, in fact, that a remote CT level is destabilized with respect to a proximate one by the smaller electrostatic interaction.

(vi) Looking at the luminescence lifetimes, there is clearly a relationship with the energy of the emitting level both at 77 K and at room temperature, as expected for radiationless processes governed by the energy gap rule.[7a,25] The relative luminescence intensities, however, are not linearly related to the luminescence lifetimes. For example, in passing from $Os(Meph\text{-}tpy)_2^{2+}$ to **1** and **4**, the luminescence intensity decreases by a factor of ~15, whereas the lifetime decreases only by a factor of ~2. This indicates that the radiative rate constant is much smaller in **1** and **4** than in the mononuclear compound. This also happens, but to a much smaller degree, for the other dinuclear species. It is clear that the interposition of a second ph spacer has a much smaller effect than interposition of the first one.

Intercomponent Energy Transfer. As we have seen in the previous section, the potentially luminescent Ru-based units do not show any appreciable emission in the dinuclear compounds (Table 3, Figures 3 and 4), indicating that they are quenched by the connected Os-based units. In order to see whether this quenching is accompanied by sensitization of the luminescence of the Os-based units, the following experiments were performed. Isoabsorptive solutions of $Os(Meph\text{-}tpy)_2^{2+}$ and of the six dinuclear compounds were excited with 650-nm light, which in the dinuclear compounds is absorbed only by the Os-based moieties (see, for example, Figure 2 and Table 1). The relative intensity values obtained for the Os-based emission are shown in Table 3. Then isoabsorptive solutions of the same compounds were excited at 500 nm, where in the dinuclear compounds approximately 50% of the absorbed light concerns the Ru-based unit (Figure 2, Table 1). The relative values of the Os-based luminescence intensity obtained under the latter experimental conditions are also shown in Table 3. One can see that the two sets of intensity values are identical within experimental error (estimated to be about 5%). This indicates that in each dinuclear compound the excitation energy absorbed by the Ru-based unit is quantitatively transferred to the connected Os-based unit.

The energy-transfer rate constant can be estimated by eq 1 or 2, where τ° and I° are the luminescence lifetime and intensity of a suitable model compound and τ and I are the Ru-based luminescence lifetime and intensity of the dinuclear compound:

$$k_{en} = 1/\tau - 1/\tau^\circ \quad (1)$$

$$k_{en} = (1/\tau^\circ)(I^\circ/I - 1) \quad (2)$$

For **3**, an appropriate model compound is $Ru(Meph\text{-}tpy)_2^{2+}$, which shows $\tau^\circ = 0.95$ ns. By using eq 1, with the estimated upper limit $\tau = 20$ ps (*vide supra*) a lower limit of 5×10^{10} s^{-1} is obtained for k_{en}. Since I° is at least 10 times larger than I, the lower limit obtained from eq 2 is 1×10^{10} s^{-1}. For **6** an appropriate model compound (e.g. $(MeO_2S\text{-tpy})Ru(tpy\text{-}phMe)^{2+}$) is not available, but from the data obtained for $Ru(MeO_2S\text{-tpy})_2^{2+}$ and $Ru(Meph\text{-}tpy)_2^{2+}$ (Table 3) one can assume that τ° is longer than 1 ns and I° is at least 3 times larger than that of $Ru(Meph\text{-}typ)_2^{2+}$ and therefore at least 30 times larger than I. Using these data, from eqs 1 and 2 one gets lower limit values of 5×10^{10} and 3×10^{10} s^{-1} for k_{en}, respectively. Since **3** and **6** are the compounds which contain the longest bridges, in the other dinuclear compounds the energy-transfer process is even faster. It is worth noticing that the energy-transfer rate constant in **3** is at least 1000 times larger than that found recently for $Ru(bpy)_3^{2+}$ and $Os(bpy)_3^{2+}$ chromophores separated by rigid nonconjugated bridges with a metal–metal distance of 17 Å.[26,27]

Energy transfer can take place by Coulombic (Förster)[28] and exchange (Dexter)[29] mechanisms. In the former one the main contribution to the rate constant comes from the dipole–dipole interaction between donor and acceptor. The rate constant according to this mechanism can be calculated from spectroscopic and structural parameters by using eqs 3 and 4:

$$k_{en} = 1/\tau^\circ(R_0/r)^6 \quad (3)$$

(25) (a) Englman, R.; Jortner, J. *Mol. Phys.* **1970**, *18*, 145. (b) Caspar, J. V.; Meyer T. J. *J. Am. Chem. Soc.* **1983**, *105*, 5583.

(26) Vögtle, F.; Frank, M.; Nieger, M.; Belser, P.; von Zelewsky, A.; Balzani, V.; Barigelletti, F.; De Cola, L.; Flamigni, L. *Angew. Chem., Int. Ed. Engl.* **1993**, *32*, 1643.

(27) De Cola, L.; Balzani, V., Barigelletti, F., Flamigni, L.; Belser, P.; von Zelewsky, A.; Frank, M.; Vögtle, F. *Inorg. Chem.* **1993**, *32*, 5258.

(28) Förster, Th. H. Discuss. Faraday Soc. **1959**, *27*, 7.

(29) Dexter, D. L. *J. Chem. Phys.* **1953**, *21*, 836.

$$R_0^6 = 5.87 \times 10^{-25}\phi^\circ/n^4 \int F(\tilde{\nu})\,\epsilon(\tilde{\nu})\tilde{\nu}^{-4}\,d\tilde{\nu} \qquad (4)$$

R_0 is the co-called critical radius, i.e. the distance at which the energy-transfer rate and the intrinsic deactivation rate of the donor are equal (50% transfer efficiency), $\tilde{\nu}$ is the frequency (cm^{-1}), and n, ϕ°, and r are the refractive index of the solvent, the luminescence quantum yield of the donor, and the donor–acceptor distance, respectively. In eq 4 the spectral overlap integral of the donor luminescence and acceptor absorption is calculated to be 9.8×10^{-14} M^{-1} cm^3 for **3**. From eq 4, R_0 is 9.1 Å for **3**, which is a value considerably smaller than the metal–metal distance (20 Å). In other words, the calculated rate constant over a 20-Å distance (eq 3) is 9.3×10^6 s^{-1}, i.e. at least 3 orders of magnitude smaller than the lower limit for the estimated experimental rate constant. It should be noted that the metal–metal distance is likely to be a structural parameter not fully appropriate for this type of calculation since the MLCT states involved in the energy-transfer process are not localized on the metals but extend considerably over the bridging ligand. For example, if the effective distance is 10 Å, the calculated rate constant would be about 100 times larger. In conclusion, it seems reasonable to admit that the Coulombic contribution could not account for the fast energy-transfer processes observed experimentally.

The Dexter-type energy transfer mechanism is described as a double exchange of electrons between donor and acceptor. Its occurrence is therefore related to direct or superexchange-mediated electronic interaction between the two partners. The rate constant of energy transfer via the Dexter mechanism can be expressed in the nonadiabatic limit as in eq 5;[30-32] ν_{en} and ΔG^* can be obtained from eqs 6 and 7, respectively:

$$k_{en} = \nu_{en} \exp(-\Delta G^*/RT) \qquad (5)$$

$$\nu_{en} = [2(H_{en})^2/\hbar](\pi^3/\lambda RT)^{1/2} \qquad (6)$$

$$\Delta G^* = (\lambda/4)(1 + \Delta G^\circ/\lambda)^2 \qquad (7)$$

Following the usual assumptions,[32-34] the free energy change ΔG° can be expressed by the difference between the spectroscopic energies of the donor and acceptor (ca. 2000 cm^{-1} for **3**, as estimated from the energy of the emission maxima of the model compounds at 77 K), and the reorganization energy λ (ca. 1000 cm^{-1}) can be estimated from the spectroscopic Stokes shift (Tables 1 and 3) of the acceptor (that for the donor should be approximately the same). This yields a value of about 0.3 for the exponential term of eq 5. In other words, k_{en} is almost equal to ν_{en}. From eq 6 it is possible to see that to obtain a ν_{en} value of 10^{10} s^{-1} (i.e., on the order of the lower limit experimentally estimated for the energy-transfer rate constant in **3**), an electronic interaction energy of less than 4 cm^{-1} (i.e., ca. 0.5 mV) is sufficient. The discussion above of the electrochemical behavior clearly shows that the interaction energy between the two moieties of **3** is likely to be much larger than 0.5 mV. Therefore, we can conclude that the very efficient electronic energy transfer observed in the examined complexes can be accounted for by a Dexter mechanism.

In conclusion, fast energy transfer takes place in our dinuclear complexes, most likely via the Dexter mechanism, even when the two $M(tpy)_2^{2+}$ chromophores are separated by two phenylene bridges. This result is consistent with the recent findings by McLendon and co-workers[18] of the small effect of phenylene spacers in decreasing electronic coupling between electron donor/electron acceptor bis-porphyrin compounds and by Mataga and co-workers[17] of fast singlet–singlet energy transfer between porphyrins through two phenylene spacers. Efficient electronic communication through phenylene bridges is also shown by the presence of intervalence bands in $(Meph\text{-}tpy)Ru^{II}(tpy(ph)_2tpy)\text{-}Ru^{III}(tpy\text{-}phMe)^{5+}$ (interaction energy ca. 170 cm^{-1})[24] and $(NH_3)_5Ru^{II}(py(ph)_2py)Ru^{III}(NH_3)_5^{5+}$.[16]

From the theoretical viewpoint, the effect of bridging phenylene spacers has been discussed by Onuchic and Beratan.[35] The basic assumption of their model is that the exchange integral within the aromatic ring is much larger than that between rings, since conjugation between the rings is broken at the ring junction due to nonbonded interactions which force the (bi)phenyl into a nonplanar geometry. In an investigation of electron transfer in bis-porphyrin compounds with different biphenylene spacers, McLendon and co-workers[18a] found that when the dihedral angle between the two phenylene spacers is varied from 0° to 50° (the known geometry of biphenyl), a 7-fold decrease in the electron-transfer rate constant is observed, in fair agreement with a decay factor of less than 10 per ring predicted by the theoretical model.[35] In terms of distance (which in the above model would not be an appropriate parameter) the rate constant for electron-transfer processes in bis-porphyrin donor/acceptor compounds with one, two, and three phenylene spacers expressed as

$$k = A_0 \exp(-\beta r) \qquad (8)$$

yielded a value of $\beta = 0.4$ $Å^{-1}$,[18b] to be compared with values around 1 $Å^{-1}$ obtained for aliphatic spacers.[36,37] Since in our compounds with $n = 0$ the electronic coupling is relatively strong, as shown by the spectroscopic and electrochemical results, introduction of one or two phenylene spacers cannot be expected to fully insulate the Ru-based from the Os-based moiety. The high rate of electronic energy transfer, therefore, is not at all surprising.

Acknowledgment. We would like to thank L. Minghetti and G. Gubellini for technical assistance. This work was supported by CNR and MURST (Italy), CNRS (France), SERC (U.K.), and SNF (Switzerland). A NATO Grant (No. 920446, Supramolecular Chemistry) is also acknowledged.

(30) Orlandi, G.; Monti, S.; Barigelletti, F.; Balzani, V. *Chem. Phys.* **1980**, *52*, 313.
(31) Closs, G.; Miller, J. R. *Science* **1989**, *244*, 35.
(32) (a) Balzani, V.; Bolletta, F.; Scandola, F. *J. Am. Chem. Soc.* **1980**, *102*, 2552. (b) Scandola, F.; Balzani, V. *J. Chem. Educ.* **1983**, *60*, 814.
(33) Ryu, C. K.; Schmehl, R. H. *J. Phys. Chem.* **1989**, *93*, 7961.
(34) Sutin, N. *Acc. Chem. Res.* **1982**, *15*, 275.
(35) Onuchic, J. N.; Beratan, D. N. *J. Am. Chem. Soc.* **1987**, *109*, 6771.
(36) Paulson, B.; Pramod, K.; Eaton, P.; Closs, G.; Miller, J. R. *J. Phys. Chem.* **1993**, *97*, 13042 and references therein.
(37) Reference 3, Chapter 5.